AD-A063 259   NORTHEASTERN UNIV BOSTON MASS ELECTRONICS RESEARCH LAB   F/G 17/9
                AN AREA INTRUSION DETECTION AND ALARM SYSTEM.(U)
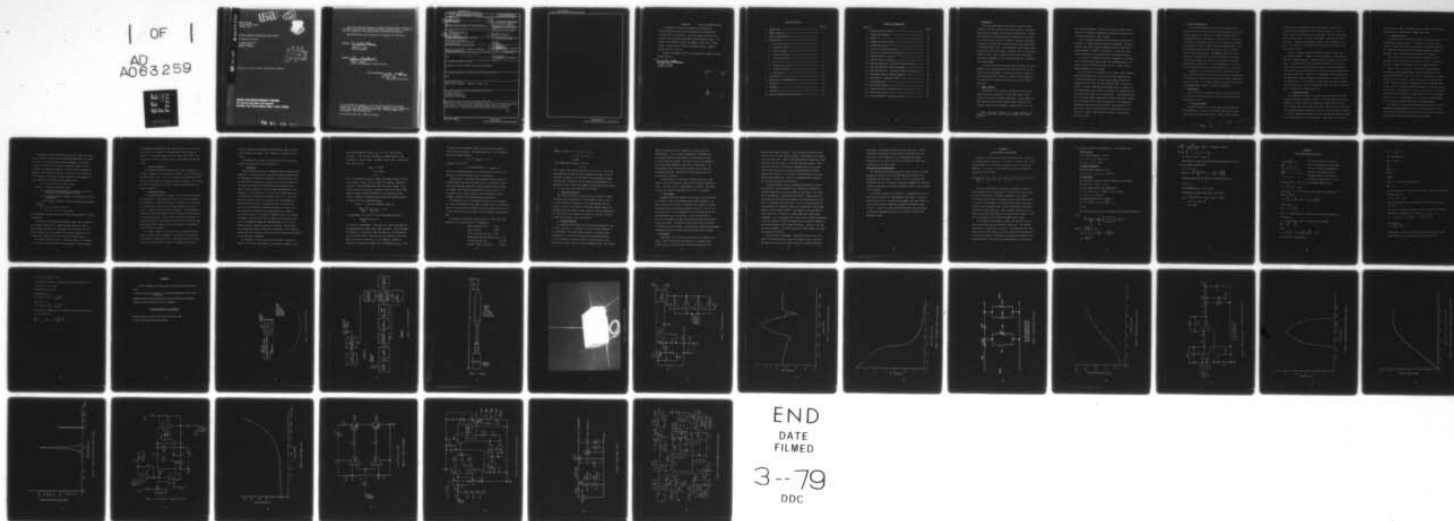   NOV 78   J S ROCHEFORT, R SUKYS, N C POIRIER   F19628-77-C-0142
UNCLASSIFIED   RADC-TR-78-258   NL

| OF |
AD
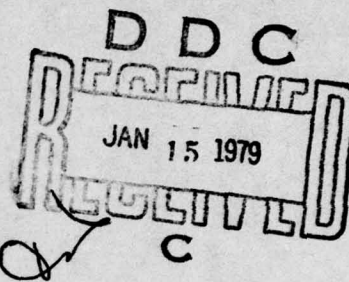A063259

END
DATE
FILMED

3--79
DDC

LEVEL II

RADC-TR-78-258
Final Technical Report
November 1978

AN AREA INTRUSION DETECTION AND ALARM SYSTEM

Northeastern University

J. Spencer Rochefort
Raimundas Sukys
Norman C. Poirier

DDC
RECEIVED
JAN 15 1979
C

ROME AIR DEVELOPMENT CENTER
Air Force Systems Command
Griffiss Air Force Base, New York 13441

79 01 12 017

This report has been reviewed by the RADC Information Office (OI) and is releasable to the National Technical Information Service (NTIS). At NTIS it will be releasable to the general public, including foreign nations.

RADC-TR-78-258 has been reviewed and is approved for publication.

APPROVED: *Nicholas V. Karas*

NICHOLAS V. KARAS
Project Engineer

APPROVED: *Allan C. Schell*

ALLAN C. SCHELL
Chief, Electromagnetic Sciences Division

FOR THE COMMANDER: *John P. Huss*

JOHN P. HUSS
Acting Chief, Plans Office

If your address has changed or if you wish to be removed from the RADC mailing list, or if the addressee is no longer employed by your organization, please notify RADC (EEC) Hanscom AFB MA 01731. This will assist us in maintaining a current mailing list.

Do not return this copy. Retain or destroy.

REPORT DOCUMENTATION PAGE		READ INSTRUCTIONS BEFORE COMPLETING FORM
1. REPORT NUMBER RADC-TR-78-258	2. GOVT ACCESSION NO.	3. RECIPIENT'S CATALOG NUMBER
4. TITLE (and Subtitle) AN AREA INTRUSION DETECTION AND ALARM SYSTEM		5. TYPE OF REPORT & PERIOD COVERED Final Technical Report 15 May 77 – 15 Feb 78
		6. PERFORMING ORG. REPORT NUMBER N/A
7. AUTHOR(s) J. Spencer Rochefort Raimundas Sukys Norman C. Poirier		8. CONTRACT OR GRANT NUMBER(s) F19628-77-C-0142
9. PERFORMING ORGANIZATION NAME AND ADDRESS Northeastern University Electronics Research Laboratory Boston MA 02115		10. PROGRAM ELEMENT, PROJECT, TASK AREA & WORK UNIT NUMBERS 62702F 46001520
11. CONTROLLING OFFICE NAME AND ADDRESS Deputy for Electronic Technology (RADC/EEC) Hanscom AFB MA 01731		12. REPORT DATE November 1978
		13. NUMBER OF PAGES 46
14. MONITORING AGENCY NAME & ADDRESS(if different from Controlling Office) Same		15. SECURITY CLASS. (of this report) UNCLASSIFIED
		15a. DECLASSIFICATION/DOWNGRADING SCHEDULE N/A

16. DISTRIBUTION STATEMENT (of this Report)

Approved for public release; distribution unlimited.

17. DISTRIBUTION STATEMENT (of the abstract entered in Block 20, if different from Report)

Same

18. SUPPLEMENTARY NOTES

RADC Project Engineer: Nicholas V. Karas (EEC)

19. KEY WORDS (Continue on reverse side if necessary and identify by block number)

Intruder Detection
Synchronous Detection
Radiating Coaxial Cable

20. ABSTRACT (Continue on reverse side if necessary and identify by block number)

This report covers the design considerations for an Area Intrusion Detection and Alarm System. The system uses a radiating coaxial cable to surround the protected area. Construction details and schematics are also included.
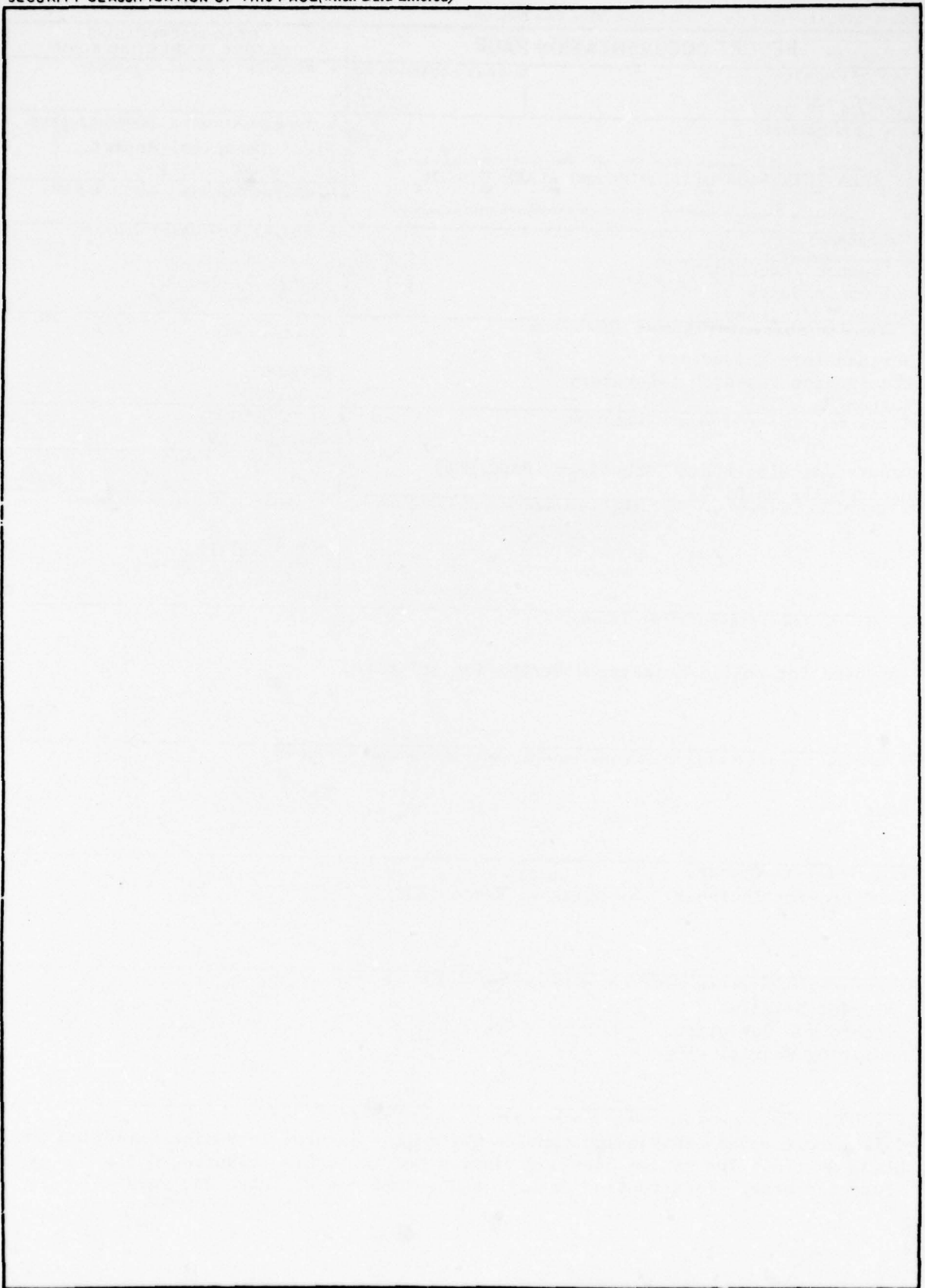
DD FORM 1 JAN 73 1473
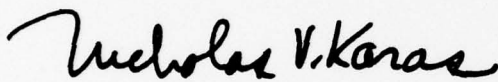
1.   The contractual efforts have produced a prototype VHF

Intruder Detection System for the protection of isolated and/or

clustered high value resources. The result meets the need of the

Air Force for a portable lightweight intruder detection system. The

system can be deployed by one or two people, within ten or fifteen

minutes, around a parked aircraft, clustered vehicles, temporary

storage area or field site.

2.   Advanced development efforts are now underway to produce a field

operable system.

NICHOLAS V. KARAS
Project Engineer

TABLE OF CONTENTS

TABLE OF ILLUSTRATIONS

1. INTRODUCTION

This report describes an area intrusion detection system intended to protect individual high value resources. The prototype system was designed, constructed and tested under a contract with the Rome Air Development Center at Hanscom Air Force Base. It is based on the ability of a receiver to detect a disturbance created by an intruder into a radio frequency field generated by a radiating coaxial cable. The development of the system closely followed the concepts set fourth in the Air Force In House Report RADC-TR-77-118[1]. These concepts were motivated by the need to improve the performance of the existing systems and to eliminate their deficiencies.

In this report the various electronic subsystems and circuits employed in the transmitting and the receiving sections of the portable prototype system are described in detail. Results of some preliminary tests conducted to observe the performance of the system and the incidence of false alarms are also briefly described.

2. GENERAL CONCEPTS

The subject of this report is an intrusion detection and alarm system which operates in the VHF range rather than at optical, infrared or microwave frequencies. Systems which have been constructed using these higher frequency detectors are adversely effected by environmental changes such as rain, fog,

---

[1]Karas, Nicholas V., Frauchi, P. R., Fante, Ronald L. and Poirier, J. Leon (1977) "An RF Intrusion Sensor for Isolated Resources."

1

snow, dust and darkness. They are also prone to develop blind spots due to shadowing of sensors by the resource being protected thus requiring multiple sensor systems.

In the frequency range chosen for this system, specifically 75.0 MHz, the above mentioned problems are minimized. The sensitivity to the size of humans is enhanced while the sensitivity to smaller animals is reduced. This leads to a lower false alarm rate and thereby to an increased overall system effectiveness.

The system is composed of five major components: the transmitter, the radiating coaxial cable, the receiving antenna, the receiver and the intrusion detection circuit. Figure 1 shows a general deployment of this system.

The basic theory of operation is as follows: the transmitter produces RF energy which is used to excite the radiating cable. The radiating cable acts as a distributed antenna system which radiates from all points to the receiving antenna. The received signal is filtered, amplified and processed in such a manner that the instantaneous received power is continuously compared with the long term time average of the received power. Any sudden departure in the received signal strength from the long term average indicates that a disturbance has occurred in some part of the signal path between the cable and receiving antenna. This disturbance, if sufficiently large, is interpreted as an intrusion and sets off the alarm. Figure 2 shows the block diagram of the intrusion detection system.

2

3. INITIAL CONSIDERATIONS

From earlier investigations and field tests performed by
the Air Force, it was found that the coupling between a receiving
antenna placed in the center of a 100 meter diameter circle of
radiating cable was in the range of -80 to -90 dBm. It was also
found that the disturbance caused by a man entering the protected
area produced a signal strength variation of approximately ±3 dBm.
The radiating cable, Type 285, used for all tests was made by
Times Wire and Cable Company. Measurements made on this cable
indicated an attenuation of 12.4 dB per 100 meters at 75 MHz,
which is approximately the same as for the common type RG-58/U
non-radiating coaxial cable. The cable impedance was 50 ohms,
as was the impedance of all the RF components used in this system.

Components for the first prototype were specified with the
aim to keep the prototype as versatile as possible. The amplifiers
purchased were wide band, low noise types with output capabilities
of up to +30 dBm. This allowed frequency and power level modifica-
tion without major changes in the circuit components.

4. SYSTEM DESIGN

In this section, a functional description of each subsystem
or circuit will be given along with their interrelationship with
the system as a whole.

A. Receiving Antenna

Several variations of vertically polarized stub antennas
were constructed. The first was a quarter wave radiating stub
with a half wave folded ground plane. These antennas exhibited

3

excellent voltage standing wave ratios with gains of approximately 6 dB in a plane perpendicular to the radiating element. This is the plane in which the radiating coaxial cable lies. The main disadvantage was its physical size. At 75 MHz, the length of the stub was approxi- one meter. (Assuming the propogation velocity in the antenna to be .92 that of free space.) This length would not allow clearance under some low profile aircraft.

The next variation reduced the height by using a loading coil in the radiating element. A length of 35 cm was found to be sufficiently short for clearance purposes. Figure 3 shows the antenna and its dimen- sions. The ground plane for this antenna is composed of the aluminum case, which houses the batteries and electronics, and four extendible radials which are stored in the base of the case and may be extended when the system is deployed. Figure 4 is a photograph of this configuration. The VSWR with the radials extended was approximately 2 and with the rad- ials stowed was 6. It is possible to operate with the radials stowed as this mismatch will not harm the transmitter output, as long as sufficient power is radiated for a good system lock.

B. Transmitter Section

The transmitter consists of a crystal controlled oscillator and an amplifier-modulator, as shown in Figure 5. The oscillator has an output frequency of 75 MHz ±.002% over a temperature range of -10°C to +60°C and an output power level greater than 0 dBm. The oscillator is followed by a wide band amplifier which has a gain of 12 dB and an output capability of +13 dBm. Amplitude modulation is produced by gating the supply voltage to the amplifier with a 1 kHz square wave. This results in an average

4

output power of +7 dBm. Transmitter power could be increased simply by replacing the amplifier with a higher power unit.

C.   Receiver Section

The receiver is a tuned RF type having no local oscillator or intermediate frequency section. It consists of a crystal filter tuned to 75 MHz, two cascaded RF amplifiers, an electronic attenuator followed by three more cascaded RF amplifiers and a tuned RF detector. Figure 2 shows the block diagram of the receiver.

The crystal filter is a four pole type designed for a 3 dB band pass of 10 kHz and has an insertion loss of 8 dB. The attenuation vs. frequency curve of the filter is shown in Figure 6.

The electronic attenuator is a wide band balanced modulator type using a Schottky diode bridge. Minimum attenuation is 2 dB and the maximum exceeds 60 dB. The curve of attenuation vs. control voltage is shown in Figure 7, and as can be seen, is extremely non-linear. Compensation for this nonlinearity will be discussed later in this report in conjunction with the description of the AGC generation circuit. This attenuator is used in the AGC loop of the receiver. Its function is to maintain a constant signal level in the intrusion detector circuit by compensating for slow drifts in received signal due to varying environment conditions and component aging.

The signal in the receiver is amplified by wide band, low noise amplifiers each having noise figures of 3.5 dB and gains of 12 dB. This low noise figure and the narrow band crystal filter are respon-sible for the rather good sensitivity of the receiver.

5

Placing the crystal filter before the first RF amplifier causes an 8 dB increase in the effective input noise power due to the insertion loss. On the other hand, the narrow bandwidth of the filter provides a protection for the first RF amplifier against possible overloads by strong nearby signals. Therefore, this configuration appears to be preferable to the one in which the filter follows the first RF stage. The effective input noise power, P_N, generated by this configuration at 290°K can be calculated from:

$$P_N = -114 \text{ dBm} + 10 \text{ Log } B + NF + \text{Losses}$$

Where P_N = effective input noise power

   B = equivalent noise bandwidth of amplifier or any filter preceding the amplifier measured in MHz

   NF = noise figure of the amplifier in dB referred to ambient temperatures

Losses = losses in cables or filters preceding the amplifier.

Therefore

$$P_N = -114 + 10 \text{ Log } .01 + 3.5 + 8$$

$$= -114 - 20 + 3.5 + 8 = -122.5 \text{ dBm}$$

For convenience the derivation of this widely used equation is included in Appendix A.

This number also represents the minimum signal level, assuming a unity signal-to-noise ratio, that the system can detect. With an average transmitter power of +7 dBm and a path loss from -80 to -90 dB, the signal level at the input to the receiver ranges from -73 to -83 dBm, well above the calculated threshold of the receiver.

The tuned RF detector circuit is shown in Figure 8. It consists of a series and a parallel tuned circuit adjusted to 75 MHz followed

by a germanium diode detector and a low pass filter set to 1.6 kHz. The output of the detector vs. RF power input curve is shown in Figure 9. The measured Tangential Signal Sensitivity (TSS) of the detector was less than -55 dBm and its 3 dB bandwidth was less than 2 MHz.

D. Band Pass Amplifier

This amplifier-filter combination has a center frequency of 1 kHz and a voltage gain of 100 at this frequency. The 3 dB frequencies are 400 Hz and 2.5 kHz. The four (4) poles of this amplifier-filter all lie on the negative real axis, giving good stability. The circuit is shown in Figure 10 and the gain - frequency characteristics are shown in Figure 11.

E. Synchronous Detector

The Synchronous Detector consists of two (2) analog gates which are driven from a 1 kHz square wave which is also used to modulate the transmitter. The circuit is shown in Figure 10. Also included in the detector is a 10 Hz low pass filter composed of R_1, R_2, C_1 and C_2. Figure 12 shows the overall amplifier - filter response to synchronous signals and Figure 13 show the rejection characteristics to asynchronous signals. This circuit is particularly helpful in rejecting signals of large amplitude that are near 75 MHz and broadband impulsive noise signals that may be generated by lightning or nearby electrical equipment.

As shown in Figure 14, the output of the synchronous detector enters a variable gain dc amplifier. The output of this amplifer is defined as "signal level" and by closed loop AGC action is maintained at the "preset level" voltage. The preset level voltage

7

drives one input of the comparator while the other input is driven by the signal level voltage. This voltage has a nominal value of 1 volt.

The signal level voltage is also used to drive the intrusion detector as well as the system lock detector.

F. AGC Circuit

The AGC Circuit consists of a comparator and a bootstrap signal generator. The rather unusual charge and discharge characteristics of this generator (Figure 15) compensate for the characteristics of the electronic attenuator and insure that the time for the AGC loop to correct a departure from the desired received signal level is nearly constant regardless of the particular operating point of the attenuator. Note that Figure 15 is plotted on a logarithmic scale. By correlating the data shown in Figures 7 and 15, it can be shown that the correction rate has a maximum value of approximately 6.8 dB per 100 second period. The particular rate of any operating point can be determined by noting the change in AGC voltage over a 100 second period centered at this operating point on Figure 15 and noting on Figure 7 the change in attenuation due to this change in voltage. This correction rate can easily track signal variation due to environmental changes and component aging, but it is slow enough to ignore variations caused by an intruder. Several alternative analog and digital schemes were considered for this long delay function, but they could not produce the proper matching characteristics for the electronic attenuator.

The operation of the AGC Circuit is as follows: referring to Figure 14, at turn on, the voltage, V_C, across the capacitor, C, is

8

zero and the generator output, V_{AGC}, is at its offset voltage,
set by R_5.   The capacitor will begin to charge through R_2 and
R_1 toward the offset voltage. The gain, at this point, is determined
by R_3 and R_4 and is:

$$V_{AGC} = 1 + R_3/R_4$$

$$= 1 + 10/100$$

$$= 1.1$$

Thus as the capacitor begins to charge, the output voltage, to which
it is trying to charge, is also rising. The capacitor voltage will
always be a fixed percentage lower than the output voltage. This
will be true until the output is clamped by the 10 volt zener diode.
Appendix B gives a detailed derivation of the operation of this
circuit. Examples of charging rates at particular operating points
are shown in the two following examples:

with V_C = .1 volt, the charging current is:

$$\frac{V_{AGC} - V_C}{10M} = \frac{.11 - .1}{10 \times 10^6} = 1 \times 10^{-9}$$

or 1 nanoampere. At a V_C of 1.0 volts the charging current is:

$$\frac{1.1 - 1.0}{10M} = 10 \times 10^{-9}$$

or a value of 10 nanoamperes. The result is an ever increasing rate
of charging until the zener diode clamps the output. The discharge of
the capacitor is controlled in much the same way. The difference is
that the effective gain of the loop from the capacitor to the other
side of the 10M is reduced from 1.1 to .9 when S_1 is gated on.
Therefore, the capacitor voltage will be 10% higher than V_{AGC}. Thus,

9

the capacitor will discharge towards an equilibrium point which is set by the offset voltage. The equilibrium point can be determined from the following equation:

$$V_C \times .9 + V_{OFFSET} \times .8 = V_C$$

solving for V_C we find:

$$V_C \text{ (at equilibrium) } = .8 \, V_{OFFSET} \times 10$$

Thus for an equilibrium point of .2 volts the offset voltage at the output of the amplifier must be set to 16 millivolts.

The gate S_1 is controlled by the comparator which compares the received signal level with the preset level. If the signal level is lower, the comparator opens the S_1 switch allowing the AGC voltage to increase, thus reducing the attenuation of the RF section. If the signal level is higher, switch S_1 closes causing the output voltage to decrease, thus introducing more attenuation.

The purpose of S_2 is to increase the speed of the AGC response by 3 orders of magnitude at the moment of system turn on. This switch stays on for 10 seconds and allows the system to come very rapidly into a "lock" condition, where the signal level and preset voltage are the same.

The range of the input RF levels in which a "lock" can be maintained may be calculated from the following data.

Power Transmitted (P_T)	+7 dBm
Path Loss (L_P)	−85 dB
Filter Insertion Loss (L_F)	−8 dB
Minimum Electronic Attenuation (L_A)	−2 dB
RF Amplifier Gain (G_A)	+65 dB
Minimum RF Input to Detector	−50 dBm

10

Signal to Detector $= P_T + L_P + L_F + L_A + G_A$

$$= 7 - 85 - 8 - 2 + 65$$

$$+ -23 \text{ dBm}$$

Excess Signal Above Minimum $= -23 + 50$

$$= 27 \text{ dB}$$

Thus a range of the input RF level for lock is 27 dB. The initial operating point can be controlled by adjusting the gain of the dc amplifier and should be set such that initial operation is toward high electronic attenuation as most likely the environmental conditions will tend to reduce the antenna coupling rather than increase it. This will have to be verified in field tests.

G. System Lock Detector

The system lock detector circuit, shown in Figure 16, senses the signal level voltage and if it lies between .9 and 1.1 volts, a red LED indicator is activated. This lamp indicates that the system is in lock. This lamp will blink when someone crosses the radiating cable indicating that the sensing circuits are operational. Of course, due to the inherent low intensity of the LED, the light can be seen only from a very short distance.

H. Intrusion Detector

The intrusion detector and alarm functions are performed by the circuit in Figure 17. It consists of a level detector composed of two comparators. The signal level voltage is ac coupled to the comparator by a 10 microfarad capacitor and one megohm resistor. This .1 Hz high pass filter and the 10 Hz low pass filter in the synchronous detector form the intrusion bandpass limits. The coupled

11

signal is compared with two voltages set by the two 500 ohm potentiometers. The two levels correspond to the extremes of the received signal variation when a ±3 dB disturbance occurs. If either level is exceeded, the output of one of the comparators will go high and trigger the 4528 one shot multivibrator. The multivibrator drives a relay whose contacts can be connected to an appropriate alarm. The relay can be wired to latch on its own contacts if required.

The multivibrator is inhibited at system turn on by a time delay to allow the operator to clear the area without tripping the alarm. The delay is set to approximately 1.5 minutes. This delay circuit can be reset by turning power off and on if required.

I. Power Supply

Throughout the system design, care was taken to avoid the need of a negative supply, thus reducing power supply complexity. As shown in Figure 18, the unit is powered by two standard 5.2 ampere-hour sealed lead acid batteries connected in series. This 18 volt pack drives two 15 volt regulators which provide isolated power to the transmitter and to the receiver. This isolation helps to prevent the modulated RF signal from directly entering the receiver on the power lines. Leakage would reduce the receiver sensitivity by masking the received signal. External power, operation and charging capabilities as well as reverse polarity protection are provided.

5. TEST RESULTS

A prototype of this system was constructed for a general evaluation. This prototype had a transmitter with variable output capabilities up to one watt and was housed separately from the

12

receiver and detection circuits. This prototype was tested success-
fully at Dover Air Force Base in November of 1978 using a C5A Aircraft
in the protected area. Several receiving antenna locations were tested
as well as the effectiveness of multiple receiving antennas. Tests
were also conducted by dividing the radiating cable into two semi-
circles and driving them as separate radiating elements through a
matched power splitter. The results of these tests are still being
analyzed and prepared for a report by a RADC/EEC group at Hanscom
Air Force Base in Bedford, Massachusetts.

In another series of tests at Northeastern University, an area
on the roof of the Dana Research Center Building was enclosed by a
radiating cable with a receiving antenna in the center. This circle
had a circumference of approximately 80 meters. Coaxial cables for
the transmitted and the received signals were connected from the roof
area to a laboratory two floors below. Due to a coupling between the
coaxial cables, the transmitter had to be transferred to the roof and
placed in a water tight enclosure. The system, in the first days of
tests, seemed very susceptible to random noise which caused false
triggering. As it was possible that this noise was internally generated,
a test was conducted in which the transmitter was directly connected to
the receiver through a 90 dB coaxial attenuator. The rest of the test
set up was unchanged. The result was that no false triggers were noted
over a period of two days.

It was found that an extreme sensitivity to wind, due to the
motion of the antenna and the cable, was a major cause of the noise.
The cable was anchored with concrete blocks and a rigid antenna was

13

constructed. This greatly reduced the false alarm rate. Further investigation determined that the elevators when operated on the upper floors were causing most of the remaining false alarms. Personnel activity on the fifth floor, just under the cable, also was detected by the test system.

CONCLUSIONS AND RECOMMENDATIONS

The operational prototype delivered to the Air Force for further testing and evaluation had an external appearance similar to the photograph shown in Figure 4. The 30 x 40 x 15 cm carrying case housing the electronics, antenna and batteries weighed nine kilograms. The battery can power the deployed system for 26 hours before recharging is required.

For further testing of the system, it is suggested that an open field area be obtained for semi-permanent cable layout. Long term tests should be run to establish false trigger rates under normal as well as adverse weather conditions, hopefully few thunder storms included. Further work should include efforts to reduce the weight and the power consumption, as well as to provide a better cable deployment method.

APPENDIX A

SIGNAL-TO-NOISE CALCULATIONS

Between the antenna and the tuned RF detector shown in Figure 2, the receiving system consists of a cascade of a crystal filter, a two stage RF amplifier, an electronic attenuator, and a three stage RF amplifier. This chain can be considered a linear RF receiver and represented as shown below.
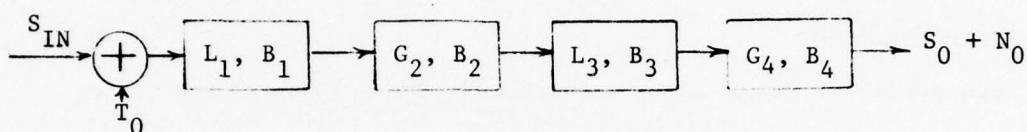
The input signal power of S_{IN} watts is presumed to come from the antenna and the only input noise is assumed to be that produced by input terminations at an ambient temperature of T_0, (290°K). The tuned Rf detector must then operate upon an output signal power of S_0 watts in the presence of an additive noise power of N_0 watts. In what follows the noise power, N_0, will be derived and defined as the effective noise power, P_N. When the output signal power, S_0, is equal to this value, the detector will operate with an SNR of 1.0 and this is presumed to be the minimum allowable value of SNR.

In the cascades shown above, L_1 and L_3 are the loss factors of the crystal filter and the attenuator respectively. The amplifier power gains are symbolized by G_2 and G_4. The equivalent noise bandwidth of the crystal filter, B_1, is much smaller than the bandwidth of the other blocks and consequently is the overall bandwidth of the receiving system. Each block can be represented by a noise figure,

15

F, and an equivalent noise temperature, T, as determined below.

CRYSTAL FILTER

Loss of 8dB, Bandwidth of 10 KHz.

$L_1 = 6.31$, $B_1 = 10^{-2}$ MHz, $F_1 = L_1$

$T_1 = T_0 (L_1 - 1) = 1540°K$

ELECTRONIC ATTENUATOR

Using minimum attenuation of 2dB,

$L_3 = 1.58$, $T_3 = T_0 (L_3 - 1) = 169.6°K$

R-F AMPLIFIERS

Each amplifier stage has a gain of 12dB and a noise figure of 3.5dB, so $G = 15.9$, $F = 2.24$.

The first amplifier has two stages and so,

$G_2 = G^2 = 251.2$, $F_2 = F + \dfrac{F - 1}{G} = 2.32$ or 3.65dB

$T_2 = T_0 (F_2 - 1) = 382.2°K$

The second amplifier has 3 stages so,

$G_4 = G^3 = 3981.3$, $F_4 = F_2 + \dfrac{F - 1}{G^2} \simeq F_2$

$T_4 \simeq T_2$

The receiving system can now be modeled by the equivalent amplifier shown:
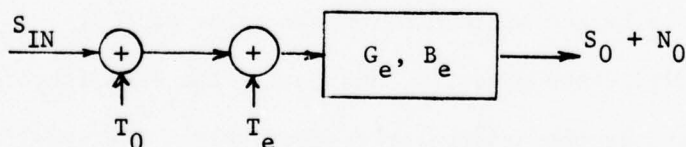
where $G_e = \dfrac{G_2 G_4}{L_1 L_3}$, $B_e = B_1$

$T_e = T_1 + L_1 T_2 + \dfrac{L_1 T_3}{G_2} + \dfrac{L_1 L_3 T_4}{G_2}$

$F_e = \dfrac{T_0 + T_e}{T_0}$

16

and $\dfrac{S_0}{N_0} = \dfrac{S_{IN}}{k(T_0 + T_e)B_1}$, where k = Boltzman's constant.

Setting $\dfrac{S_0}{N_0} = 1$, and $P_N = N_0 = S_{IN}$

$$P_N = k(T_0 + T_e)B_1 = k\,T_0\,F_e\,B_1$$

When numerical values are substituted in the expression for T_e, it can be readily verified that

$$T_e \simeq T_1 + L_1\,T_2$$

Then $F_e = \dfrac{T_0 + T_1 + L_1\,T_2}{T_0} = 1 + \dfrac{T_1}{T_0} + L_1\left(\dfrac{T_2}{T_0}\right)$

Substituting for $\dfrac{T_1}{T_0}$ and $\dfrac{T_2}{T_0}$,the expression reduces to

$$F_e = L_1\,F_2$$

and consequently $P_N = k\,T_0\,L_1\,F_2\,B_1$

Expressing B_1 in MHz and P_N in mW, we may write

$P_{dB} = 10\,\text{Log}\,(10^9 k\,T_0) + L_{1dB} + F_{2dB} + 10\,\text{Log}\,B_1$

$\qquad = -114 + 8 + 3.65 - 20$

$\qquad = -122.4$ dBm

17

APPENDIX B

AGC Voltage Generator Analysis
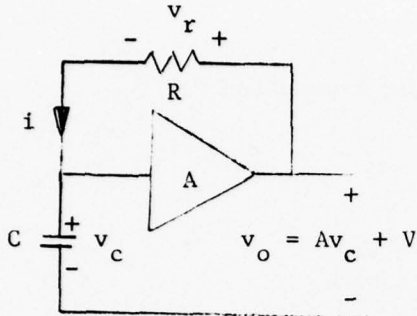
The bootstrap circuit of Figure 14 may be represented by the equivalent circuit shown in the accompanying drawing. Interpretation of the parameters shown is a function of the status of the switch S_1 in the original circuit. When S_1 is in the high impedance state

$$A = 1 + \frac{R_3}{R_4} \quad \text{and} \quad V = V_{OFS}.$$

Where V_{OFS} is the offset voltage at the output of 3140 amplifier. When S_1 conducts

$$A = \left(1 + \frac{R_3}{R_4}\right)\left(\frac{R_7}{R_2 + R_7}\right) \quad \text{and} \quad V = V_{OFS}\frac{R_7}{R_2 + R_7}.$$

In both cases

$$v_{AGC} = v_c \left(1 + \frac{R_3}{R_4}\right).$$

Also, it is assumed that no current flows in the input terminals of the amplifier.

The equivalent circuit is governed by the equation

$$\frac{dv_o}{dt} = \frac{dv_r}{dt} + \frac{dv_c}{dt}$$

Since

$$v_r = iR, \quad \frac{dv_c}{dt} = \frac{i}{C} \quad \text{and} \quad \frac{dv_o}{dt} = \frac{Adv_c}{dt} = \frac{A}{C}i$$

this equation is equivalent to

18

$$\frac{A}{C} i = R \frac{di}{dt} + \frac{i}{C}$$

and consequently to

$$\frac{di}{dt} + \frac{1 - A}{RC} i = 0$$

or

$$\frac{di}{dt} + \frac{i}{\tau} = 0$$

where

$$\frac{RC}{1 - A} = \tau$$

When $A = 1$, this equation reduces to

$$\frac{di}{dt} = 0$$

and the solution $i = I$ = constant is obtained. Therefore, the output voltage is a ramp

$$v_o = v_c = \frac{I}{C} t = \frac{V}{RC} t$$

When $A \neq 1$ the solution of the differential equation is given by

$$i = Ke^{-t/\tau}$$

where K is a constant determined by initial conditions. Therefore, evaluated at an arbitrary $t = 0$ when $v_c = V_C$ and $v_o = V_O$

$$K = i = \frac{V_O - V_C}{R} = \frac{V + AV_C - V_C}{R} = \frac{V + (A - 1) V_C}{R}$$

and therefore

$$i = \frac{V + (A - 1)V_C}{R} e^{-t/\tau}$$

Integrating to obtain the voltage across the capacitor and substituting $\frac{RC}{1 - A}$ for τ to achieve simplification, we obtain

$$V_C = \left(V_C - \frac{V}{1 - A}\right) e^{-t/\tau} + K_1$$

To evaluate the constant of integration K_1 we note that at $t = \infty$

$i = 0$ and $V_C = V_0 = AV_C + V$

consequently $K_1 = \dfrac{V}{1 - A}$

Therefore when $A < 1$

$$V_C = \frac{V}{1 - A} + \left(V_C - \frac{V}{1 - A}\right) e^{-t/\tau}$$

and when $A > 1$

$$V_C = \frac{V}{1 - A} + \left(V_C - \frac{V}{1 - A}\right) e^{+t/\tau}$$

The capacitor charging rate at an arbitrary operating point where $v_c = V_C$ is given by

$$\left.\frac{dv_c}{dt}\right|_{t' = 0} = \frac{i}{C} = \frac{V + (A - 1)V_C}{RC}$$

20

PERSONNEL

A list of engineers who contributed to the work reported is given below:

J. Spencer Rochefort, Professor of Electrical Engineering, Co-Principal
                      Investigator

Raimundas Sukys, Senior Research Associate, Co-Principal Investigator

Norman C. Poirier, Research Associate, Engineer.

RELATED CONTRACTS & PUBLICATIONS

F19628-77-C-0142, 15 May 1977 through 15 February 1978

No other publications have been issued.

RECEIVING
ANTENNA

XMTR | RCVR+ALARM

PROTECTED AREA
INSIDE CIRCLE
DEFINED BY
RADIATING
CABLE

CERT 285
RADIATING CABLE

RG-58 COAXIAL CABLE

50Ω
TERMINATION
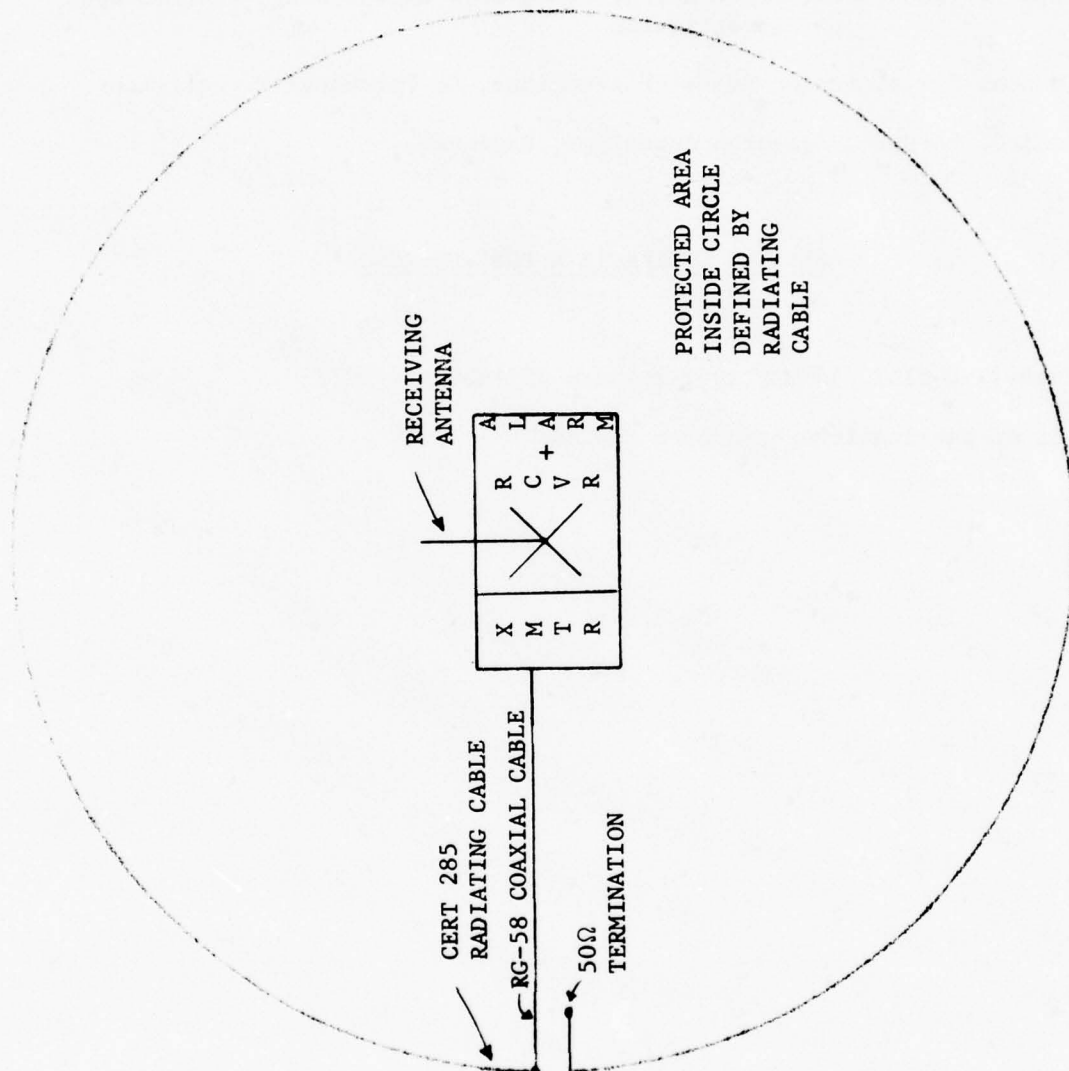
Figure 1 - General Layout Of System

Radiating
Cable
Antenna

75 MHz
Oscillator

RF
Amplifier
Modulator

TRANSMITTER

RECEIVING
ANTENNA

Crystal
Filter

RF
Amplifier

Electronic
Attenuator

RF
Amplifier

Tuned
RF
Detector

Modulation
Oscillator

Bandpass
Amplifier
Synchronous
Detector

AGC
Detector

Intrusion
Detector

RECEIVER
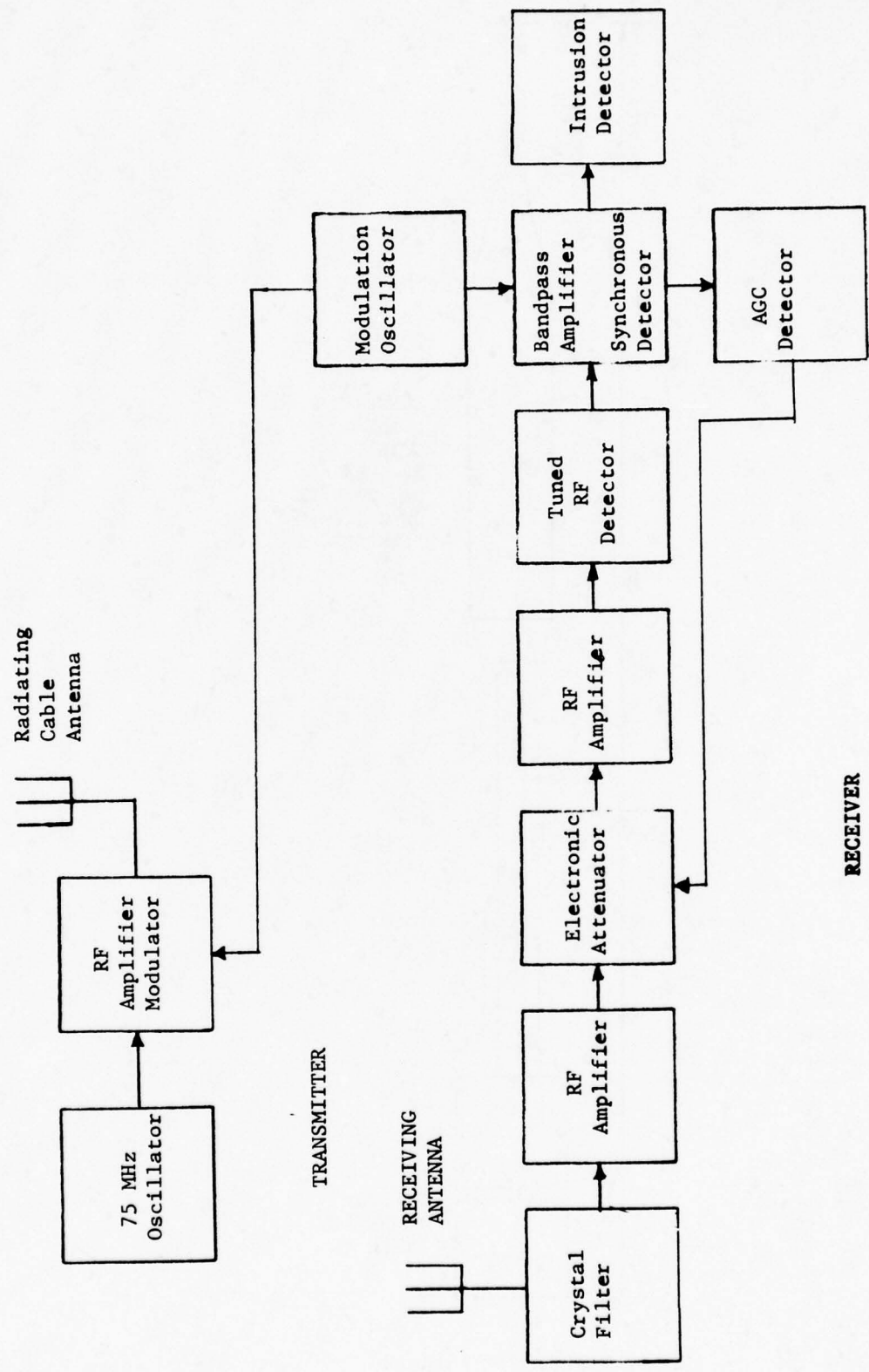
Figure 2 – System Block Diagram

CENTER
LOADING
COIL
22 TURNS
NO. 20 WIRE
ON A 1 CM
DIAMETER FORM

14.7 CM

35 CM

UG 628A
CONNECTOR
(TYPE C)

Figure 3 - Antenna

24
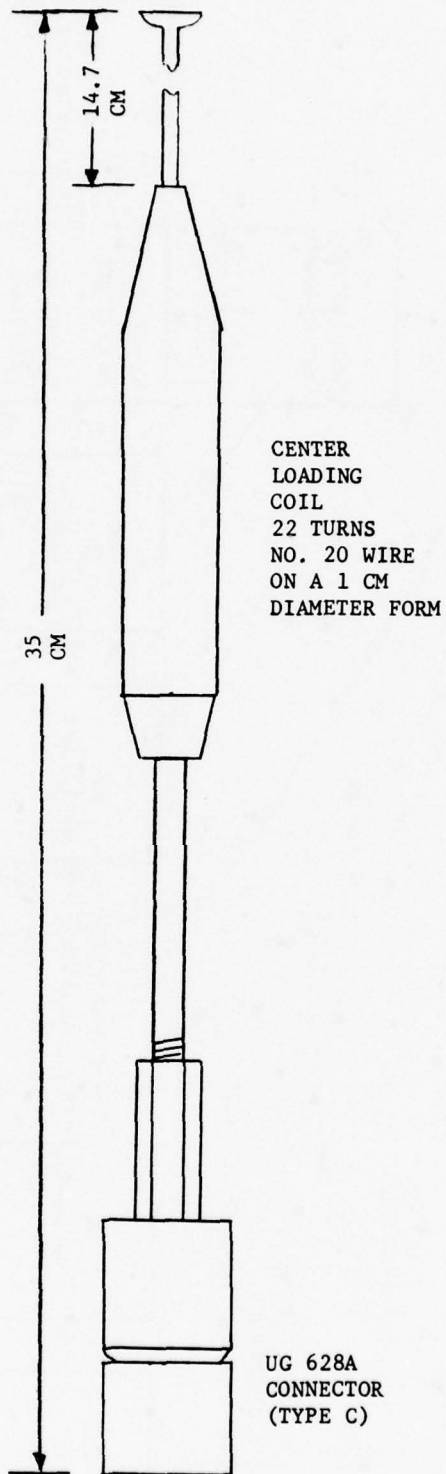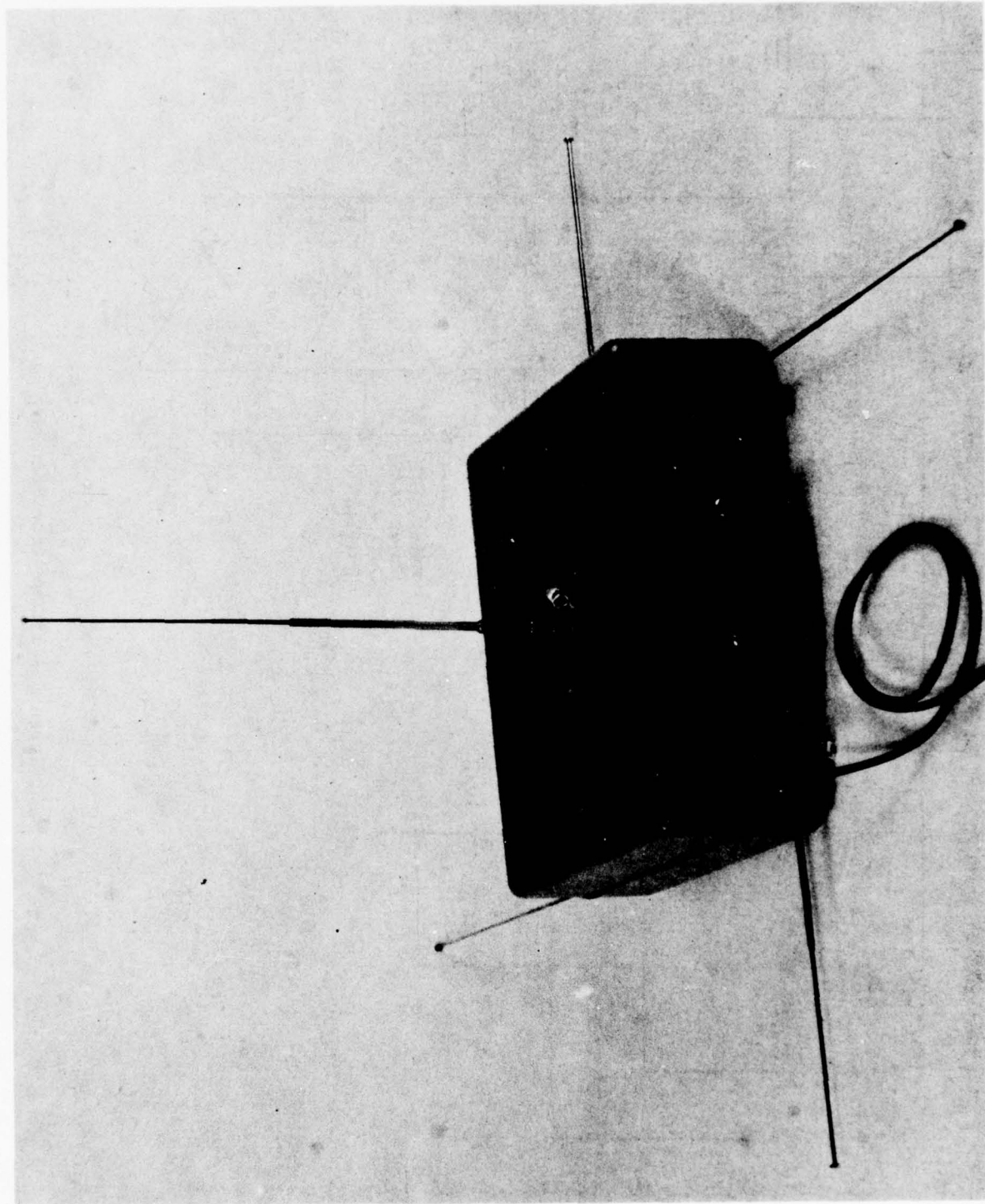
Figure 4 — Antenna With Ground Plane

25
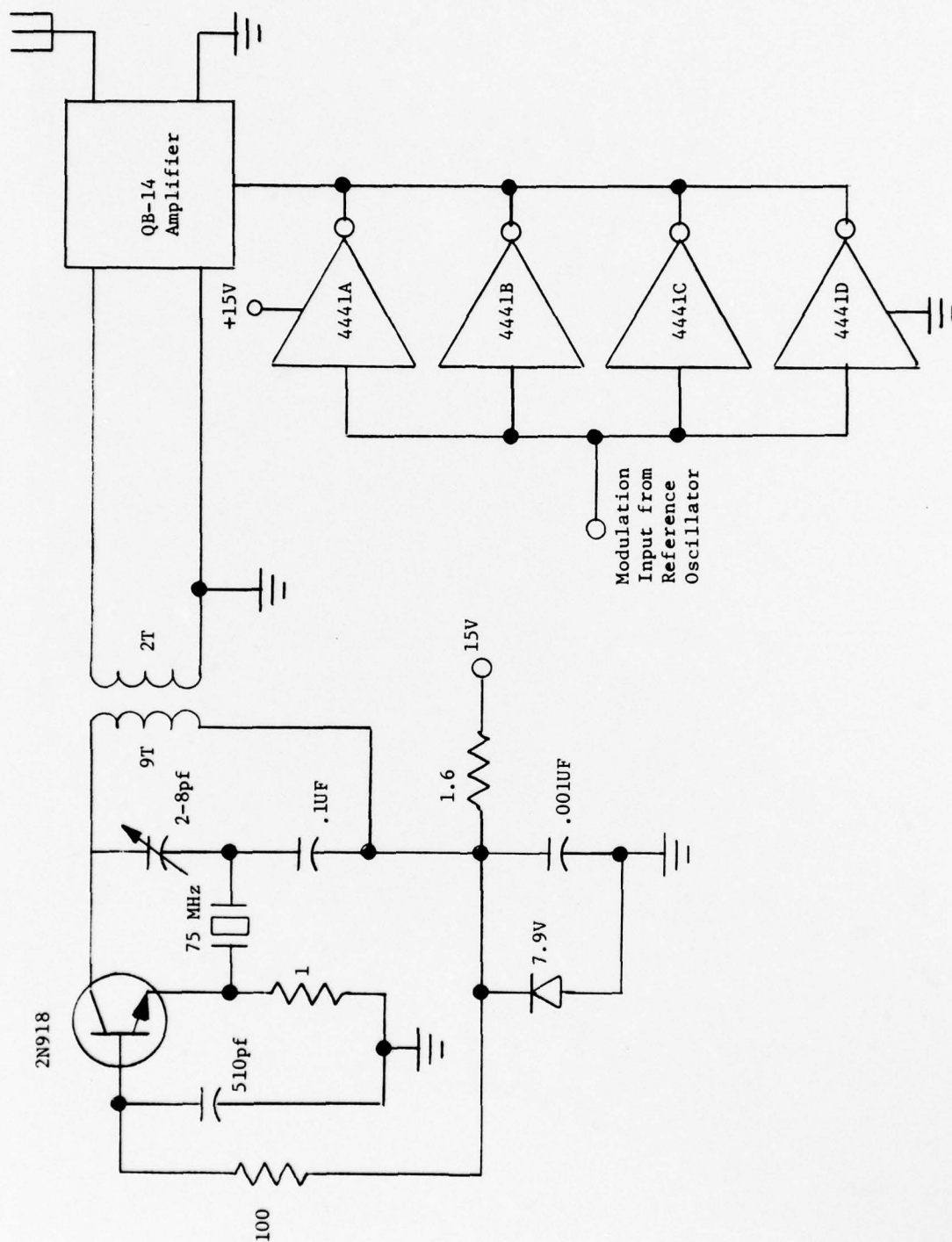
Figure 5 - Transmitter Section

26

FREQUENCY (MHz)

ATTENUATION (DB)
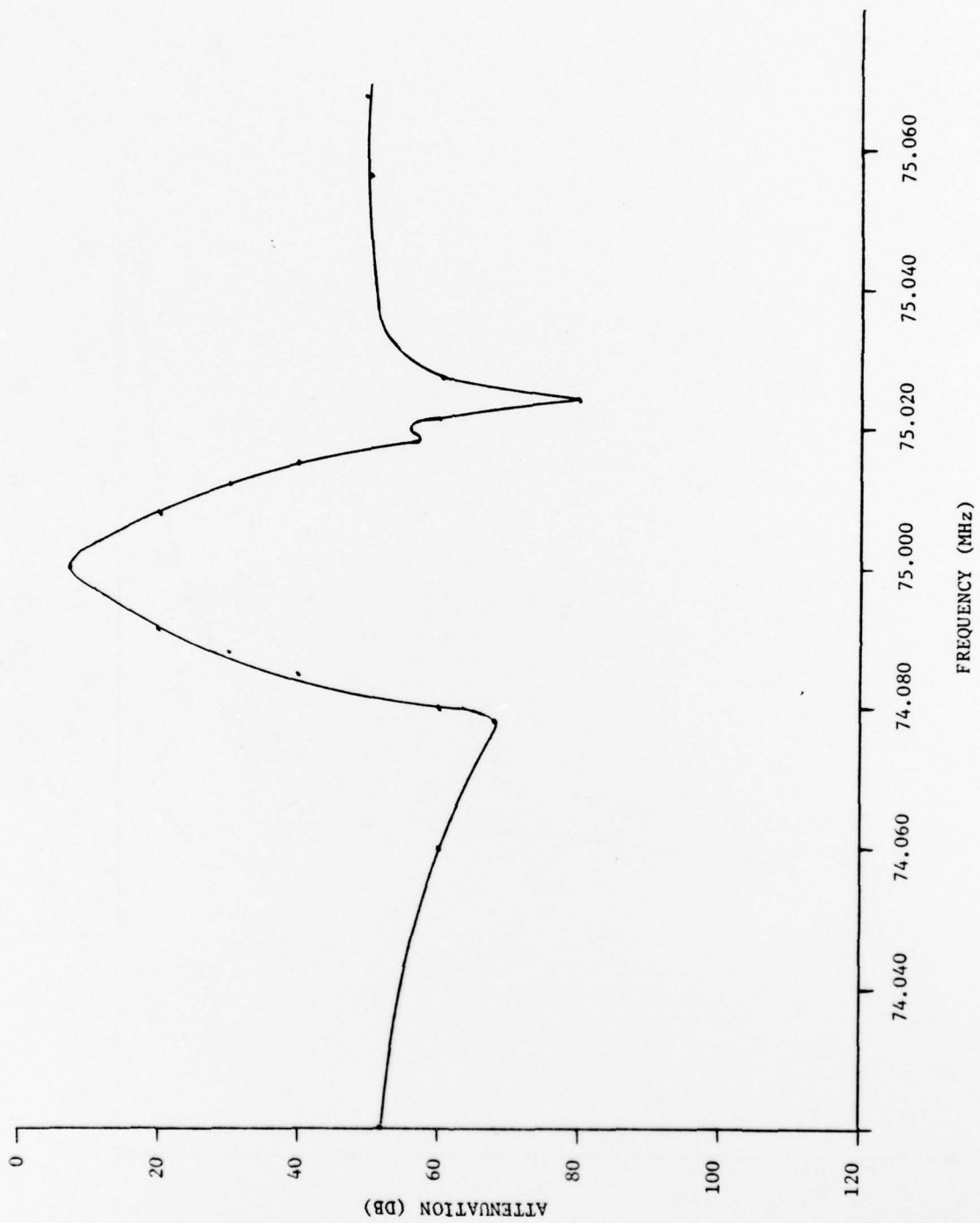
Figure 6 - Crystal Filter Characteristics

27
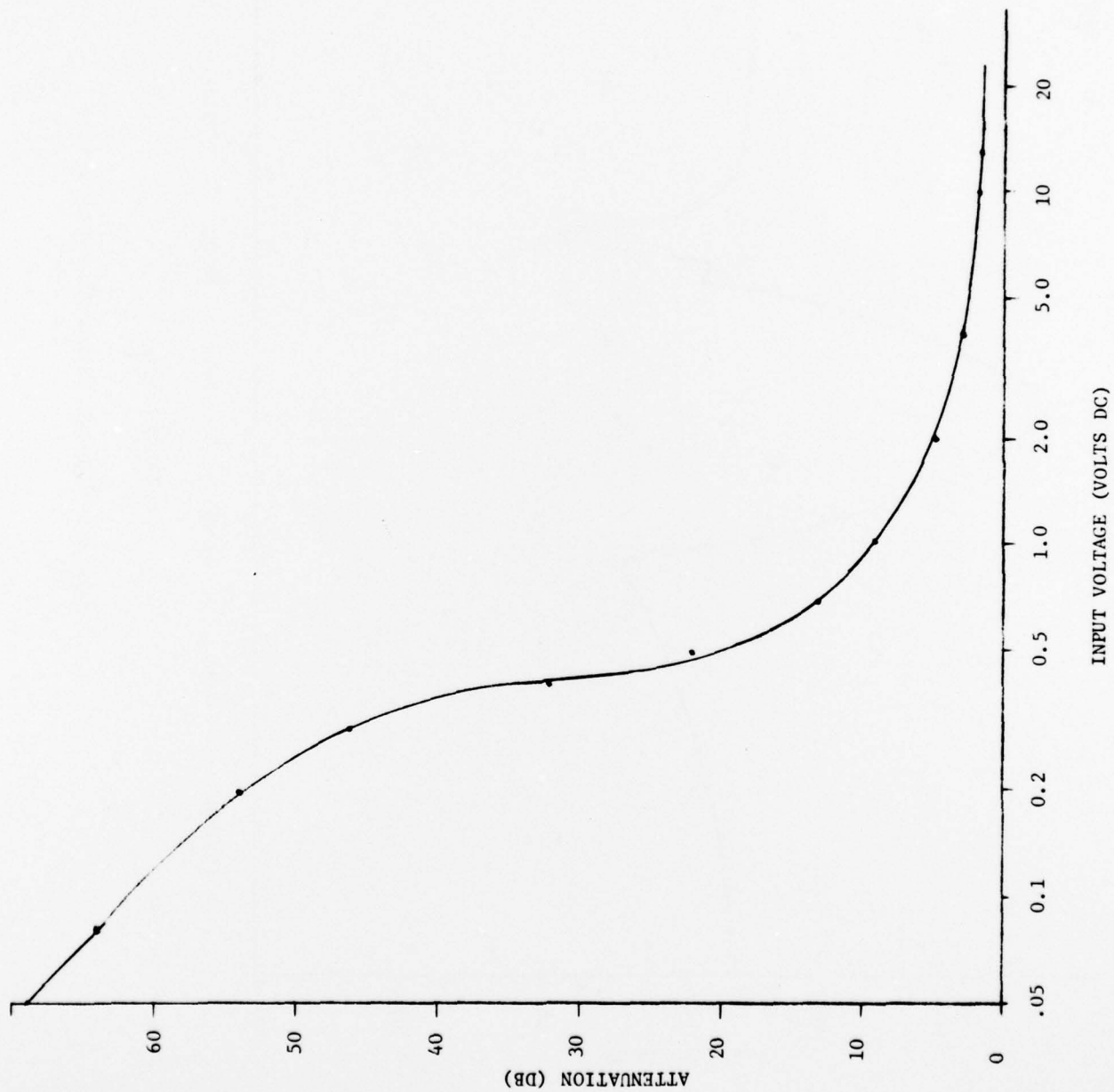
Figure 7 - Electronic Attenuator Characteristics

28

OUTPUT

1 MEG

100PF

1 - 10PF

IN276

1 - 10pf

3UH

3UH

INPUT
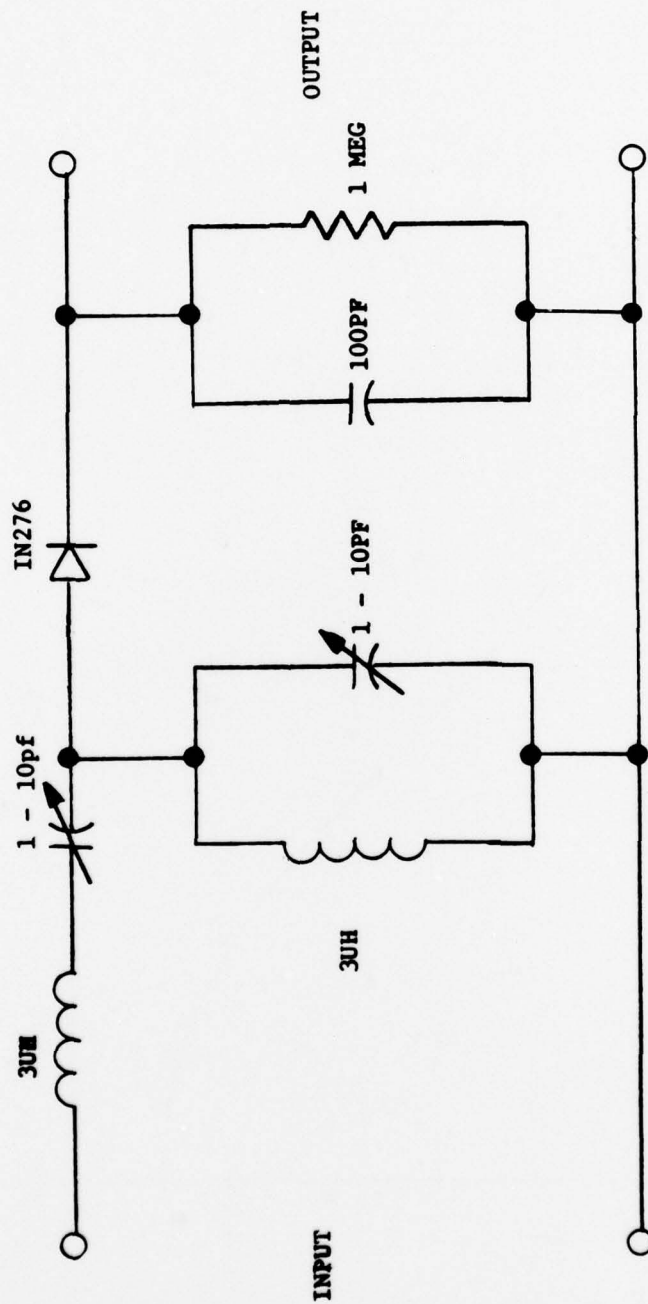
All the resistors in kΩ
All the capacitors in μF
unless otherwise noted.

Figure 8 - Tuned RF Detector Circuit

29
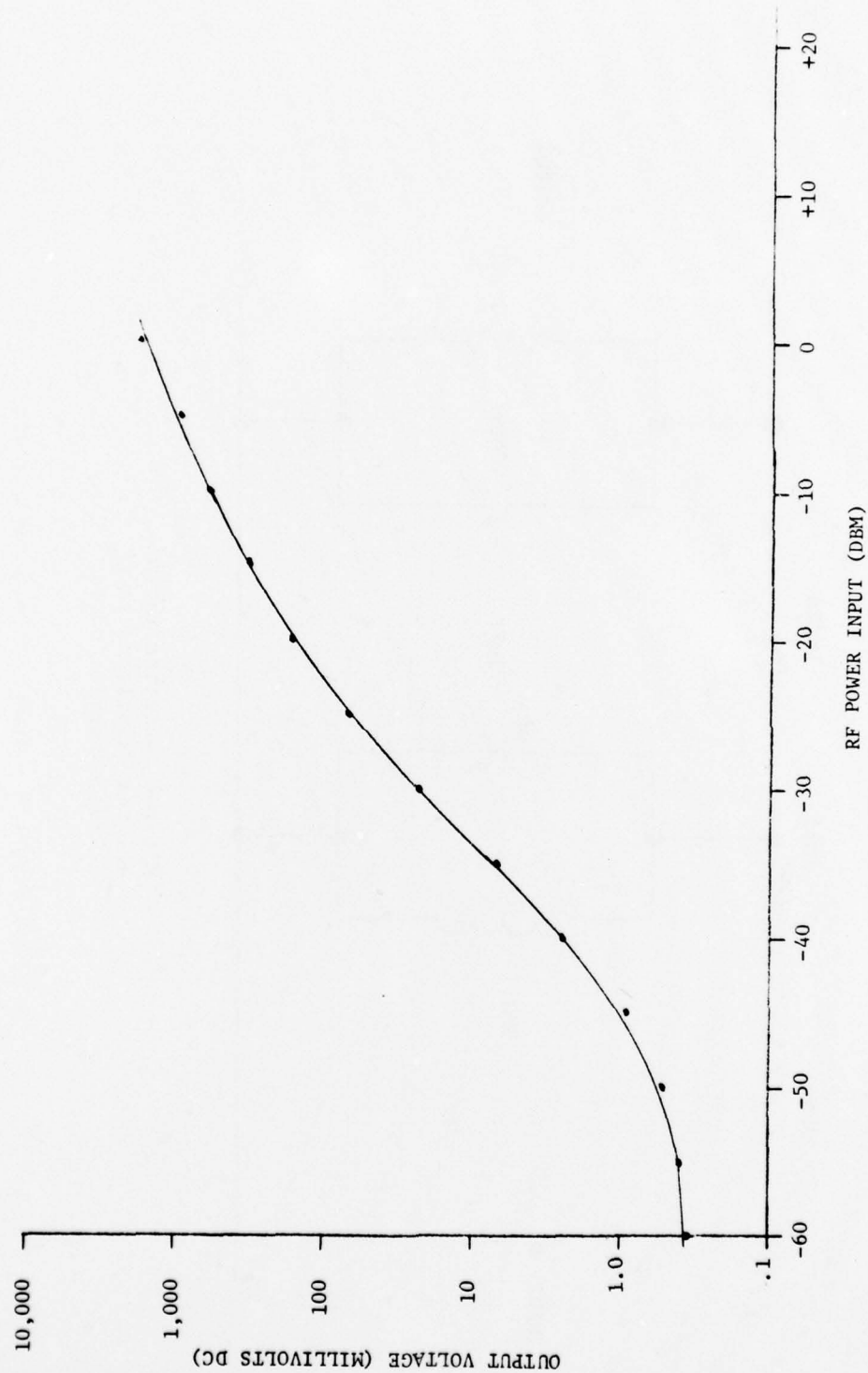
Figure 9 - Tuned RF Detector Sensitivity
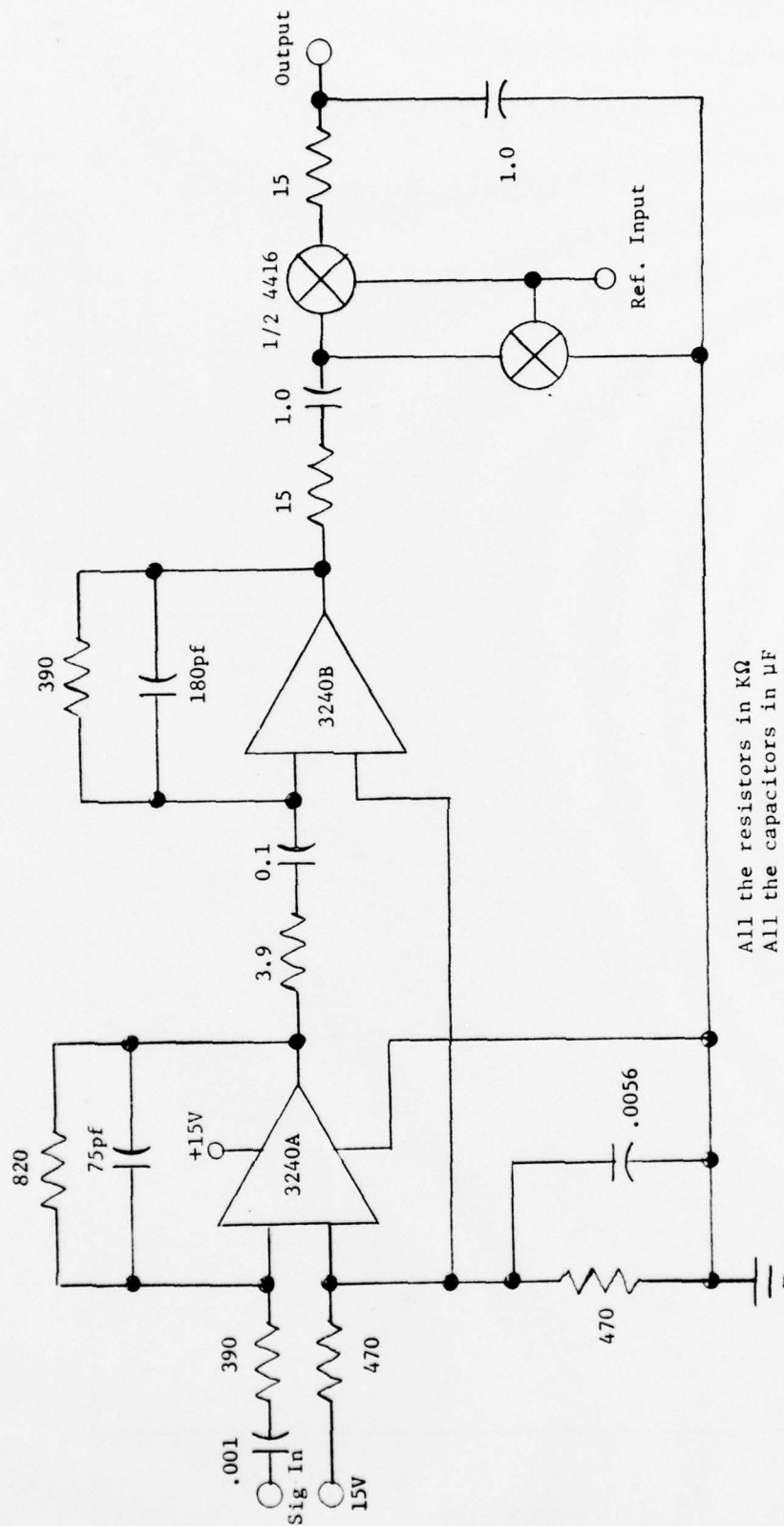
Figure 10 - Band Pass Amplifier - Synchronous Detector Circuit

All the resistors in KΩ
All the capacitors in μF
unless otherwise noted.
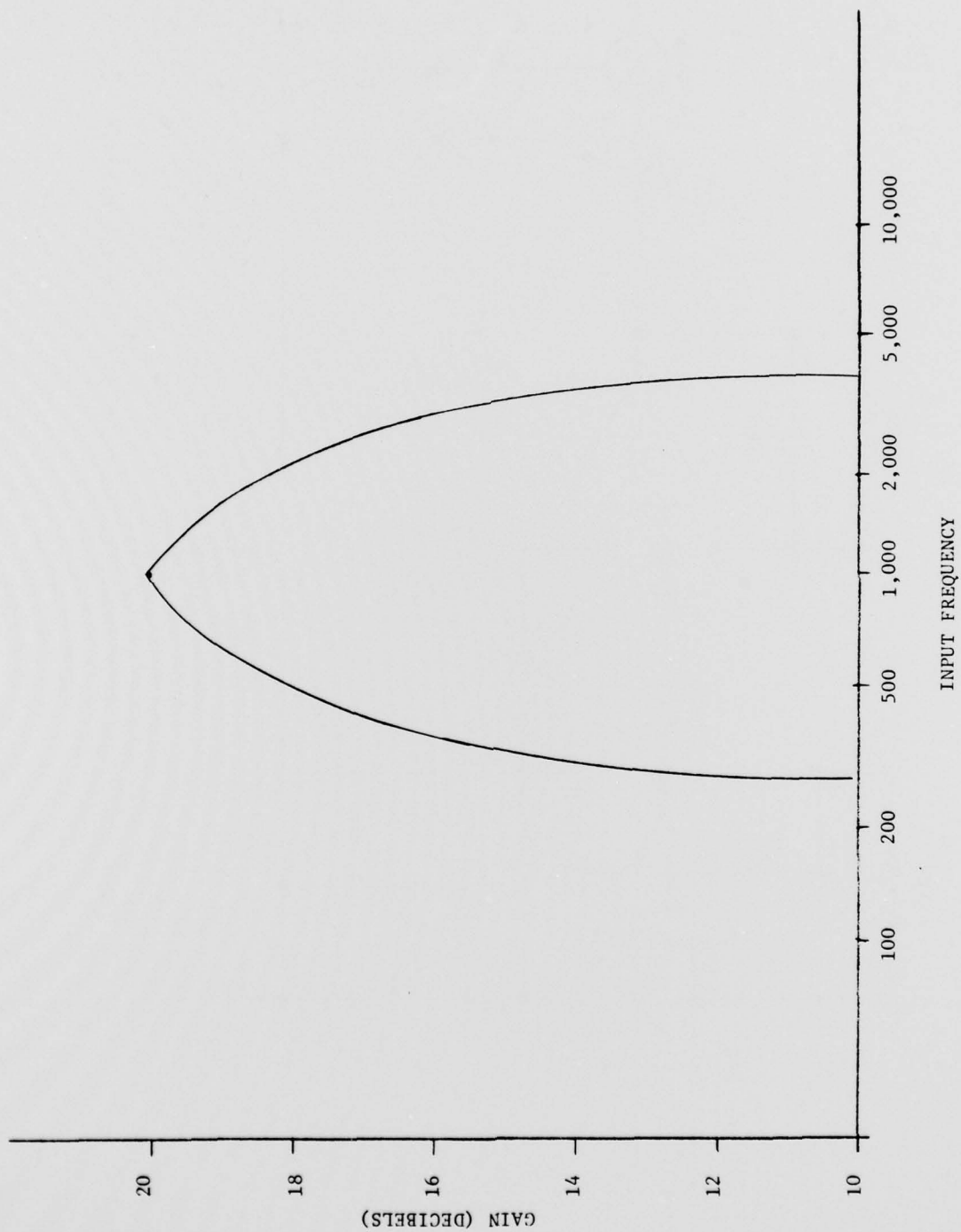
Figure 11 – Band Pass Amplifier Frequency Response

32

INPUT VOLTAGE AT 1.0 KHz (VOLTS PEAK TO PEAK)

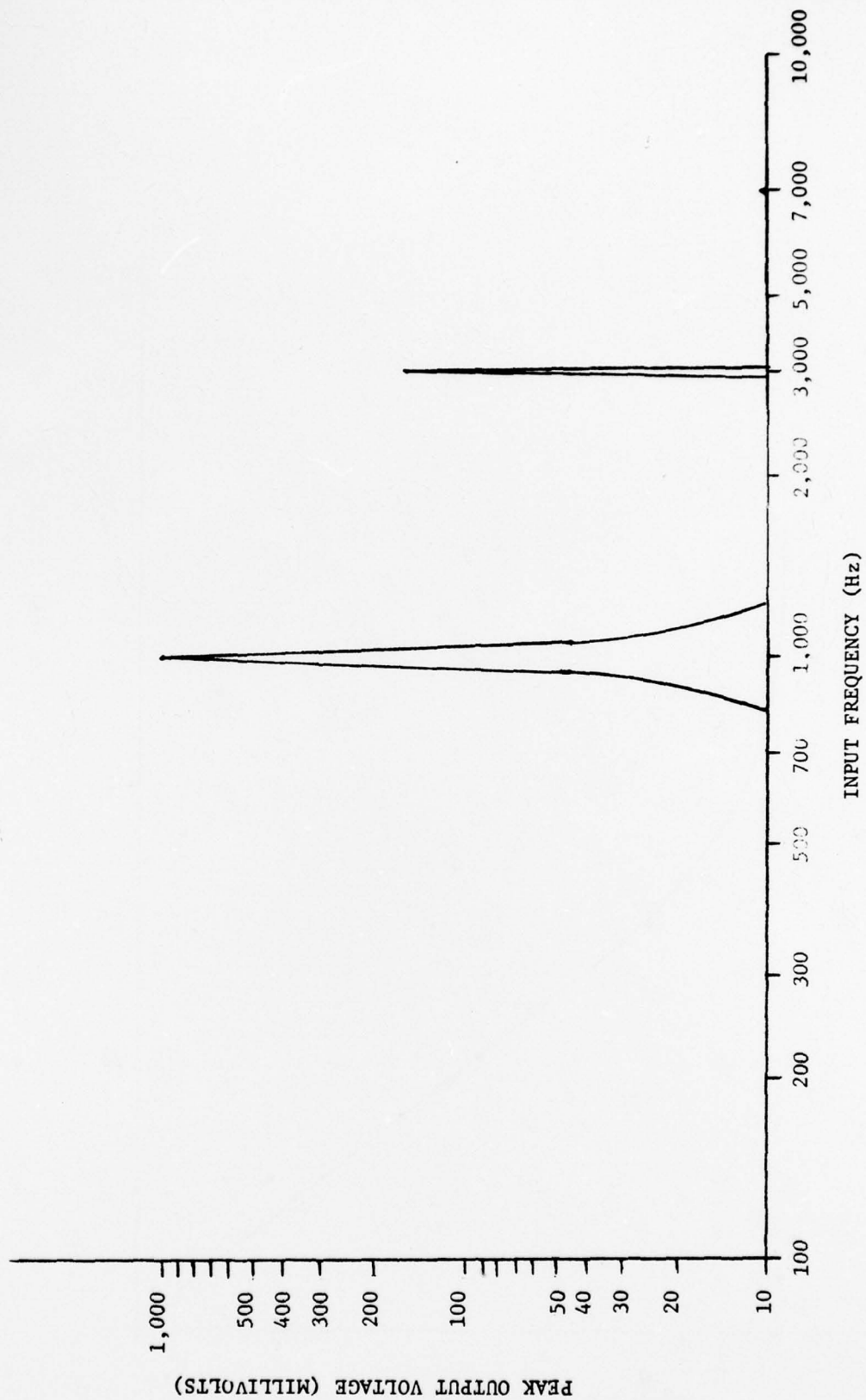Figure 12 - Band Pass Amplifier - Synchronous Detector Sensitivity

OUTPUT VOLTAGE (VOLTS DC)

Figure 13 - Synchronous Detector Frequency Response

INPUT FREQUENCY (Hz)

PEAK OUTPUT VOLTAGE (MILLIVOLTS)

100

10

+15V

3140

2

AGC OUT
To Voltage
Controlled
Attenuator

510

OFFSET

2

10M

10

9.2UF

From
Start
Delay

AGC
Ramp
Generator

10

1/4 4416

10V

Gain
Adj

100

10

+15V

Signal
Level

3230A

3230B

Input from
Synchronous
Detector

COMPARATOR

10

+15V

1

Preset Level
(1 volt)
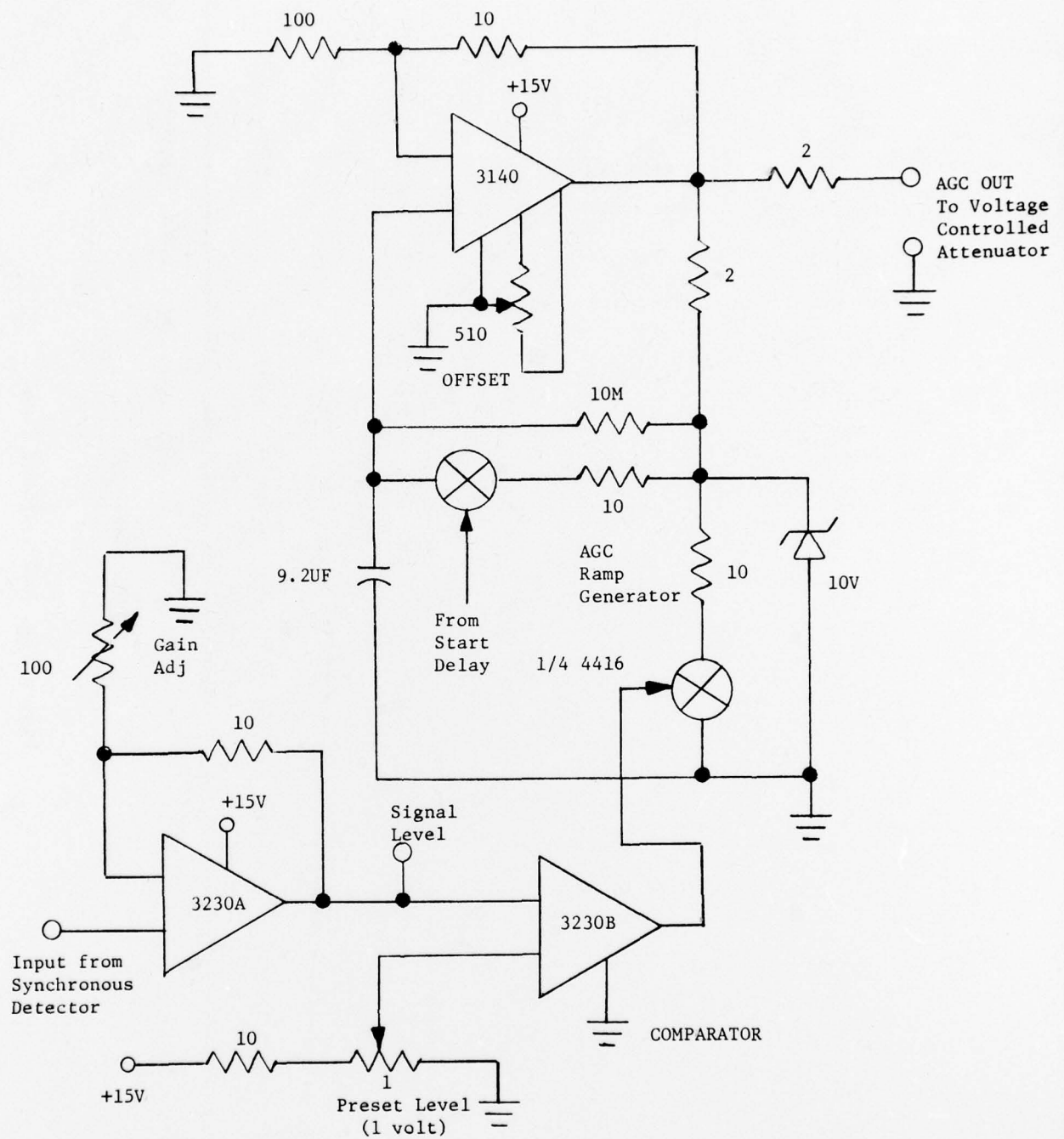
Figure 14 - AGC Amplifier - Generator Circuit
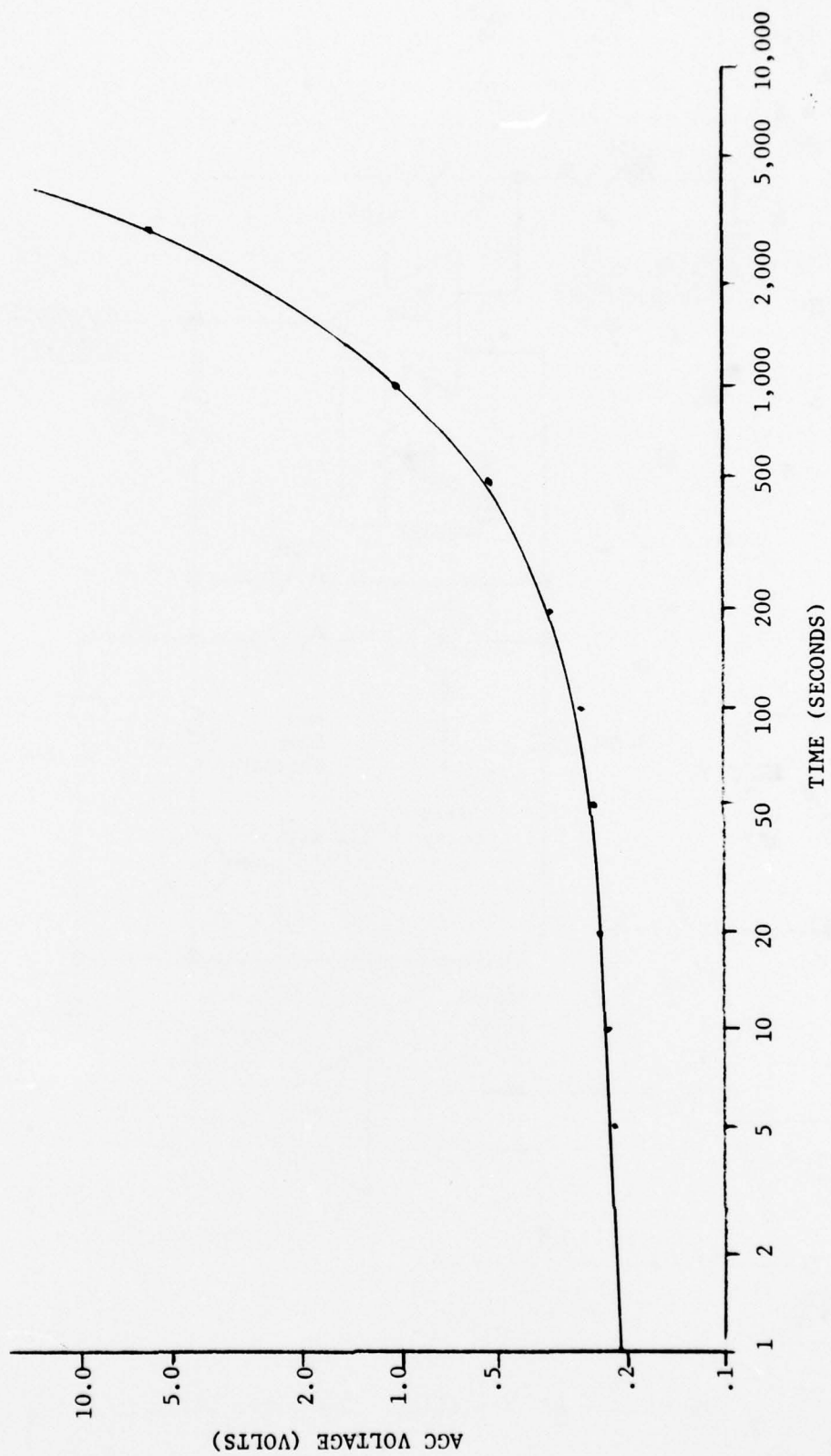
Figure 15 - AGC Response Time

36

All the resistors in KΩ
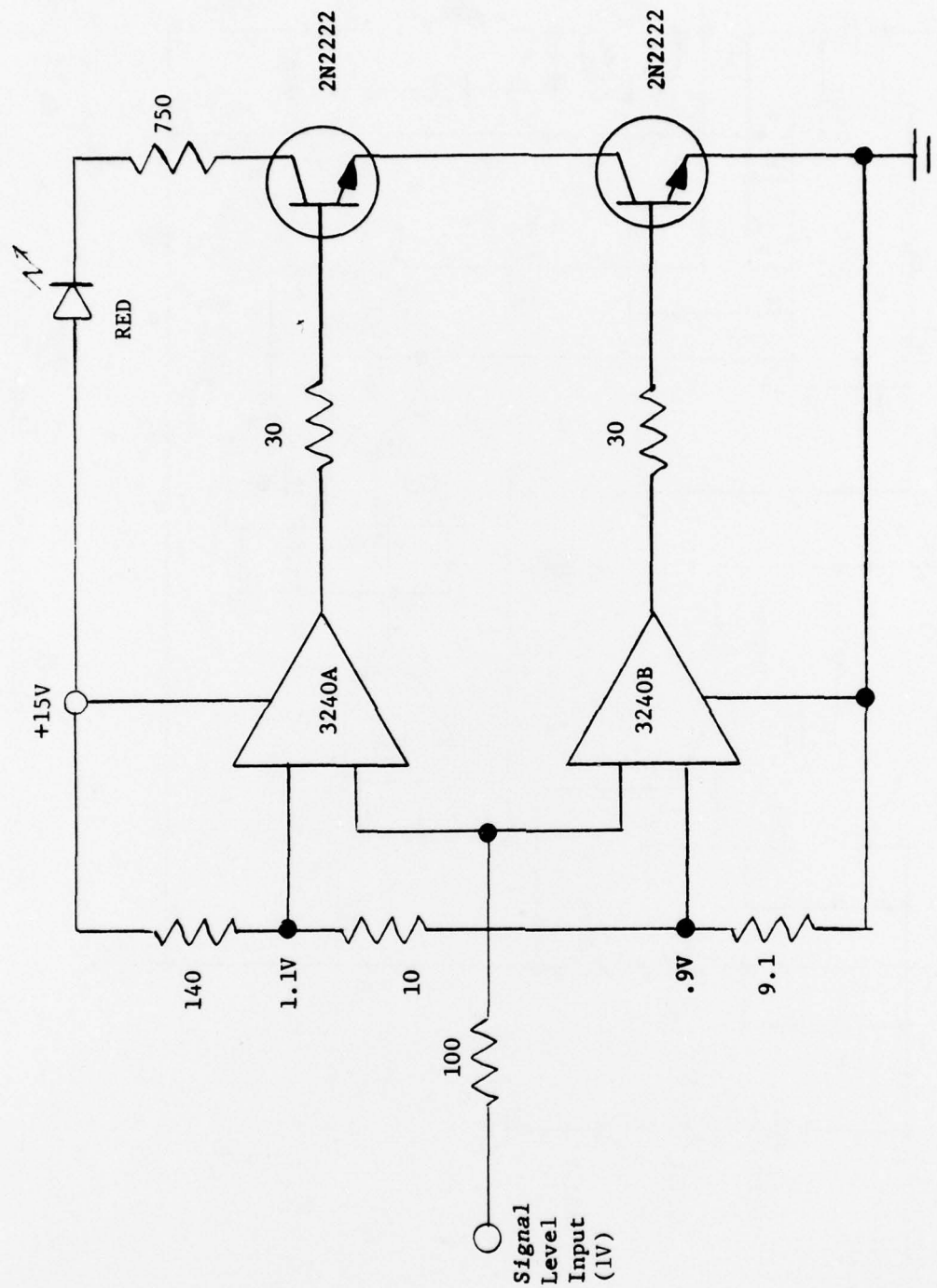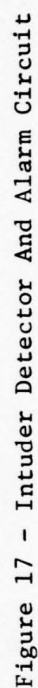
Figure 16 – System Lock Detector

37

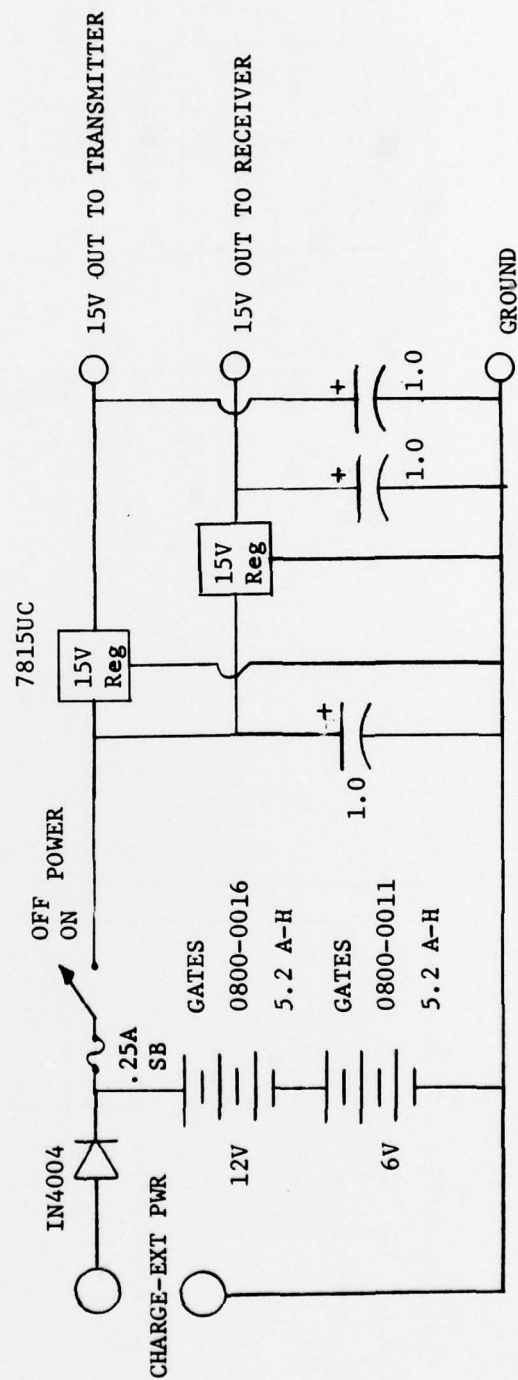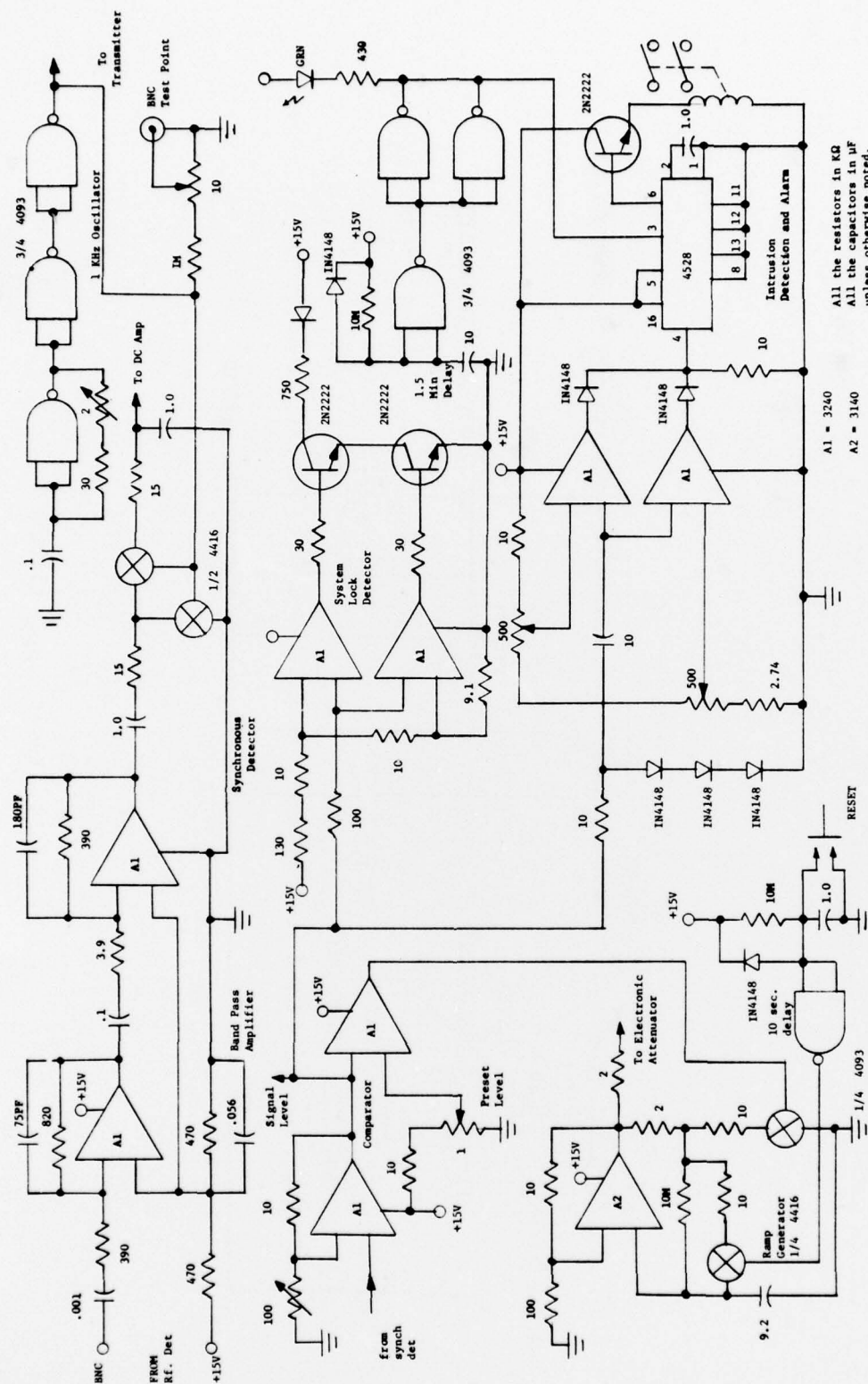Figure 17 - Intuder Detector And Alarm Circuit

38

Figure 18 - Power Supply Circuit

Figure 19 – Overall Schematic Of Detection System